www.katwacollegejournal.com
e-ISSN 2455-5916 | Vol. X | Issue 2 | Dec 2025
Katwa College
Peer Reviewed
International Journal of Research on
Social and Natural Sciences

Mathematical Modelling of Covid-19 Dynamics using a Prey Predator Framework for Healthcare Capacity and Infection Rates

Samir Tamang[1]

[1]Assistant Professor, Department of Mathematics, Vivekananda Mahavidyalaya, Purba Bardhaman, 713103, West Bengal, India.

Email: samirtamang81@gmail.com

Article Received: **Oct 12, 2025** | Revised Ariticle Received: **Nov 21, 2025** | Final Acceptance: **Dec 3, 2025**

Abstract

The COVID-19 pandemic required strong epidemiological models to understand and predict disease spread. The traditional Susceptible-Infected-Recovered (SIR) model, though fundamental, frequently overlooks real-world intricacies. Studies emphasize the possibility of integrating prey-predator dynamics, drawn from the Lotka-Volterra model, to provide a deeper insight into COVID-19 transmission by framing the connection between susceptible people and the virus (or infected individuals) as a predator-prey dynamic. Here in this modelling, we take infected population as prey and the healthcare capacity as the predator. In normal COVID-19 models we have seen that healthcare capacity can be an important part as when the healthcare capacity is low and infection rate is high then there is an out spurge in the mortality rates. Here we wish to choose the healthcare capacity as the constant parameter and try to understand the infection rates considering different scenario.

Keywords

Prey-predator models; Stability; Functional response.

1. Introduction

The COVID-19 pandemic, has profoundly transformed global health and societal perceptions regarding the dynamics of infectious diseases [1,2,3,4]. The swift and extensive spread of the virus underscored the urgent necessity for advanced epidemiological models to effectively evaluate, forecast, and ultimately manage the transmission of the disease. Mathematical modelling techniques emerged as essential instruments for comprehending the fundamental dynamics of the virus and formulating effective public health strategies, including social distancing protocols, vaccination initiatives, and targeted allocation of resources [3]. F. Kangalgil, N. Topsakal & O. Kuzucu [5], discussed about the

local dynamics of a discrete-time COVID-19 pandemic and it found that under some parametric conditions, the discrete-time model has two equilibrium points. Furthermore Neriman Kartal, S. Kartal [6] investigated Maximum Lyapunov exponents which shows the complex dynamics of COVID-19. Asini A. Konpola, G. S. Chathurika & I.G. Udagedara [11] also worked in the Evolution of COVID-19 disease using a one prey two predator model where infected considered as prey and recovered and death classes are considered as predator. Dunn, P. R. & Hovel, K.A., [9] studied similar situation with marine habitats where the type of predator influences the frequency of functional response. The good number of studies has been published taking SIR model [1 – 8, 10 – 16,18] which enumerated that the actual transmission of COVID-19 revealed considerable heterogeneity and individual variability, with a relatively small fraction of infected individuals responsible for a disproportionately large number of secondary cases (superspreading events).

To get the detailed idea of the spread of the disease, we take a traditional SIR model and present a more nuanced view of COVID-19 transmission dynamics, this proposal suggests the integration of prey-predator dynamics, inspired by the classic Lotka-Volterra model, into the SIR framework. This methodology conceptualizes the interaction between susceptible individuals and the virus (or infected individuals) as a predator-prey relationship. In this analogy, infectious are the "prey" whose numbers are diminished by the "predator," which in this context signifies the healthcare capacity. This integration seeks to more accurately capture the complexities of the transmission dynamics. In this variation of a prey-predator model for COVID-19, the relationship is inverted to explore the dynamics from a different perspective. This model can examine how the availability and use of healthcare resources influence the infection's spread and severity.

Here the **prey (infected)** is represented by the population of individuals currently infected with COVID-19. The growth of this population is initially exponential and is constrained by the availability of uninfected individuals.

The **Predator (Healthcare Capacity)** is represented by the healthcare system's capacity, including ICU beds, ventilators, and staff. As a "predator," the healthcare system reduces the prey population by treating and curing infected individuals.

The infected population is reduced by the "predation" of the healthcare system. The rate at which the healthcare system "consumes" infections depends on both the number of infected individuals and the capacity of the system. Recovered Individuals who have recovered from COVID-19 and are assumed to have temporary or permanent immunity. Infected individuals can recover and return to the susceptible or recovered compartments, creating a feedback loop between the disease and the susceptible population.

We treat the healthcare system's capacity as a parameter and its changes are based on **Strain from infections.** When the infected population grows, it strains healthcare resources. This is modelled as a negative effect on healthcare capacity, analogous to how a predator population declines if its food source is scarce. Also, its changes depend on **Growth of capacity.** In response to the growing prey population (infection), healthcare capacity can expand through measures like building field hospitals, redeploying staff, or increasing funding. This can be modelled as proportional to the number of infected people, with some upper limit. And the last it depends on the **baseline capacity and decay.** The system maintains a certain baseline capacity, and capacity can decay over time as resources are depleted or staff burn out.

2. Model formulation

We take the following variables:

$S(t)$: Susceptible individuals

$I(t)$: Infectious (active cases)

$R(t)$: Recovered/ Removed

Here we consider healthcare capacity not a dynamic variable in the ODE system, instead we treat it as a parameter or externally-specified function of time to get a better understanding of the transmission rate with the healthcare capacity in the prey-predator framework. Hence, we have the following model.

$$\frac{dS}{dt} = \Lambda N - \beta \frac{SI}{N} - \delta S \quad (1)$$

$$\frac{dI}{dt} = \beta \frac{SI}{N} - \gamma I - aHI - \delta I \quad (2)$$

$$\frac{dR}{dt} = \gamma I + aHI - \delta R \quad (3)$$

Where $\beta =$ Transmission rate (per day)

$\gamma =$ Baseline recovery rate (per day)

$a =$ per unit healthcare effort for maximum treatment rate or per unit effectiveness.

$H =$ Healthcare capacity

$\Lambda =$ Recruitment rate through birth or immigration into S.

$\delta =$ Natural death rate (per capita)

The term aHI indicates the treatment rate or removal rate by the healthcare capacity per day.

Where $a =$ per unit healthcare effort for maximum treatment rate or per unit effectiveness. Which can be translated as $F(I,H) = aHI$ is the number of infected cured per individual healthcare facility. As $\boldsymbol{a}$ is the searching rate or effort, with the increase in the value of $\boldsymbol{a}$ the number of individuals being cured also increases proportionally. The inclusion of aHI means higher healthcare effort and capacity reduce the infectious population, promoting stability. Here we will study the effect of health care capacity and effort and see how it influences the dynamics. The healthcare capacity (H) is a predator here and it consumes cases through treatment, quarantine or hospitalization limiting further transmission and reducing the effective reproduction rate.

3. Equilibrium points

For critical points, $\frac{dS}{dt} = 0 = \frac{dI}{dt} = \frac{dR}{dt}$ (4)

Therefore, $\Lambda N - \beta \frac{SI}{N} - \delta S = 0$; $\beta \frac{SI}{N} - \gamma I - aHI - \delta I = 0$ and $\gamma I + aHI - \delta R = 0$

$\Rightarrow$ $\Lambda N - \beta \frac{SI}{N} - \delta S = 0$ (5)

$\beta \frac{SI}{N} - \gamma I - aHI - \delta I = 0$ (6)

$\gamma I + aHI - \delta R = 0$ (7)

3.1. Disease-free equilibrium

For disease free equilibrium, there are no infected individuals, i.e. $I = 0$.

From equation (5), we have $\Lambda N - \beta \frac{SI}{N} - \delta S = 0$

$$\Rightarrow \quad \Lambda N - \delta S = 0 \quad \Rightarrow \quad S = \frac{\Lambda N}{\delta}$$

Again, from equation (7), we get $\delta R = 0 \quad \Rightarrow \quad R = 0$

So, the disease-free equilibrium is $E_0(S^*, I^*, R^*) = \left(\frac{\Lambda N}{\delta}, 0, 0\right)$,

It means only the susceptible population in non-zero and its value depends on the recruitment and natural death rates, while infected and recovered populations are zero.

3.2. Endemic equilibrium

The endemic equilibrium is the steady state where the disease persists in the population, i.e. when $I \neq 0$.

Let the endemic equilibrium point be $E_0(S^*, I^*, R^*)$, then we have

$$\Lambda N - \beta \frac{S^* I^*}{N} - \delta S^* = 0; \tag{8}$$

$$\beta \frac{S^* I^*}{N} - \gamma I^* - aHI^* - \delta I^* = 0 \tag{9}$$

$$\gamma I^* + aHI^* - \delta R^* = 0 \tag{10}$$

From equation (9), we get $I^* \left(\beta \frac{S^*}{N} - \gamma - aH - \delta\right) = 0$

$$\Rightarrow \beta \frac{S^*}{N} - \gamma - aH - \delta = 0$$

$$\Rightarrow S^* = \frac{N(\gamma + aH + \delta)}{\beta} \tag{11}$$

From equation (8), we get $\beta \frac{S^* I^*}{N} = \Lambda N - \delta S^* \Rightarrow I^* = \frac{N(\Lambda N - \delta S^*)}{\beta S^*}$

$$\Rightarrow I^* = \frac{N\left(\Lambda N - \delta \frac{N(\gamma + aH + \delta)}{\beta}\right)}{\beta} \times \frac{\beta}{N(\gamma + aH + \delta)} \Rightarrow I^* = \frac{\Lambda N - \delta \frac{N(\gamma + aH + \delta)}{\beta}}{\gamma + aH + \delta} \tag{12}$$

Similarly, from equation (10), we get $R^* = \frac{I^*(\gamma + aH)}{\delta} \quad \Rightarrow R^* = \frac{I^*(\gamma + aH)}{\delta}$

$$\Rightarrow R^* = \frac{\Lambda N - \delta \frac{N(\gamma + aH + \delta)}{\beta}}{\gamma + aH + \delta} \times \frac{(\gamma + aH)}{\delta} \tag{13}$$

Now, here the infection per unit time is given by $\beta \frac{SI}{N}$ and the rate at which the individual leaves the infectious compartment is $\gamma + aH + \delta$. So, the infected individual can produce $\beta \frac{S}{N}$ new infectives.

As initially, I is negligible at the beginning and $S \cong N$, the basic reproduction number is, $R_0 = \frac{\beta}{\gamma + aH + \delta}$

So, if $R_0 < 1$, the disease-free equilibrium is locally stable and the infection cannot invade and if $R_0 > 1$, the disease-free equilibrium is unstable and the infection may spread. Here we can see that R_0 is dependent on the term aH, which means that there is stabilizing effect of health care intervention.

4. Stability Analysis

The Jacobian matrix of the given system, with variables S, I, R is given by

$$J = \begin{pmatrix} \frac{\partial f_1}{\partial S} & \frac{\partial f_1}{\partial I} & \frac{\partial f_1}{\partial R} \\ \frac{\partial f_2}{\partial S} & \frac{\partial f_2}{\partial I} & \frac{\partial f_2}{\partial R} \\ \frac{\partial f_3}{\partial S} & \frac{\partial f_3}{\partial I} & \frac{\partial f_3}{\partial R} \end{pmatrix} \quad \text{where} \quad \begin{aligned} f_1 &= \Lambda N - \beta \frac{SI}{N} - \delta S \\ f_2 &= \beta \frac{SI}{N} - \gamma I - aHI - \delta I \\ f_3 &= \gamma I + aHI - \delta R \end{aligned}$$

$$\Rightarrow J = \begin{pmatrix} -\frac{\beta I}{N} - \delta & -\frac{\beta S}{N} & 0 \\ \frac{\beta I}{N} & \frac{\beta S}{N} - \gamma - aH - \delta & 0 \\ 0 & \gamma + aH & -\delta \end{pmatrix} \qquad (14)$$

4.1. Stability analysis at $E_1(S^*, 0, 0)$

At the disease-free equilibrium, we have $S^* = \frac{\Lambda N}{\delta},\ I^* = 0$

Therefore, from equation (14), we get the Jacobian matrix at disease free equilibrium (J_1), as,

$$J_1 = \begin{pmatrix} -\delta & -\frac{\beta\Lambda}{\delta} & 0 \\ 0 & \frac{\beta\Lambda}{\delta} - \gamma - aH - \delta & 0 \\ 0 & \gamma + aH & -\delta \end{pmatrix} \qquad (15)$$

Therefore, the eigen values are $\lambda_1 = -\delta,\ \lambda_2 = \frac{\beta\Lambda}{\delta} - \gamma - aH - \delta$ and $\lambda_3 = -\delta$

Clearly $\lambda_1, \lambda_3 < 0$, thus, the system is locally asymptotically stable around $\boldsymbol{E_1(S^*, 0, 0)}$ if $\frac{\beta\Lambda}{\delta} - \gamma - aH - \delta < 0$

Hence the system is stable around a critical point $\boldsymbol{E_1(S^*, 0, 0)}$, when $\frac{\beta\Lambda}{\delta} < \gamma + aH + \delta$.

i.e. when $\frac{\beta\Lambda}{\delta(\gamma + aH + \delta)} < 1$

4.2. Stability analysis of $E_2(S^*, I^*, R^*)$

At endemic equilibrium, we have $I^* \neq 0$, so from equation (9) we have,

$$\beta \frac{S^*}{N} - \gamma - aH - \delta = 0 \Rightarrow \beta \frac{S^*}{N} = \gamma + aH + \delta$$

Let us denote $K = \gamma + aH + \delta$ for simplicity. Then we can write the above equation as $\beta \frac{S^*}{N} = K$.

Also, from equation (12) we have, $I^* = \frac{\Lambda N - \delta \frac{N(\gamma + aH + \delta)}{\beta}}{\gamma + aH + \delta} = \frac{\Lambda N}{K} - \frac{\delta N}{\beta} = \frac{N}{K\beta}(\Lambda\beta - \delta K)$ (16)

Since, $R_0 = \frac{\beta}{K}$, equation (16) can also be written as, $I^* = \frac{N}{\beta}(\Lambda R_0 - \delta) = \frac{\delta N}{\beta}\left(\frac{\Lambda}{\delta} R_0 - 1\right)$

Then the Jacobian matrix, equation (14), can be written as

$$J_2 = \begin{pmatrix} -\left(\frac{\beta I^*}{N} + \delta\right) & -K & 0 \\ \frac{\beta I^*}{N} & \frac{\beta S^*}{N} - K & 0 \\ 0 & \gamma + aH & -\delta \end{pmatrix} \Rightarrow J_2 = \begin{pmatrix} -\left(\frac{\beta I^*}{N} + \delta\right) & -K & 0 \\ \frac{\beta I^*}{N} & 0 & 0 \\ 0 & \gamma + aH & -\delta \end{pmatrix} \qquad (17)$$

The eigen values of J_2, are given by $det(J_2 - \lambda I) = 0$, so we have,

$$\begin{vmatrix} -\left(\frac{\beta I^*}{N} + \delta\right) - \lambda & -K & 0 \\ \frac{\beta I^*}{N} & \frac{\beta S^*}{N} - K - \lambda & 0 \\ 0 & \gamma + aH & -\delta - \lambda \end{vmatrix} = 0 \qquad (18)$$

Since the matrix (17), is block triangular, from the bottom right block, one of the eigen-value is $\lambda_3 = -\delta$, which is a negative value. The other two eigen-value can be calculated from the top-left (2x2)-block of J_2.

i.e. $$A = \begin{pmatrix} -\left(\frac{\beta I^*}{N} + \delta\right) & -K \\ \frac{\beta I^*}{N} & 0 \end{pmatrix} \quad (19)$$

The characteristic equation of the matrix A is, $\lambda^2 - (Trace\ (A))\lambda + Det(A) = 0$,

Where $Trace(A) = -\left(\frac{\beta I^*}{N} + \delta\right) + 0 = -\left(\frac{\beta I^*}{N} + \delta\right)$ and $Det(A) = \frac{\beta I^*}{N}(K)$,

Then the characteristic equation becomes $\lambda^2 + \left(\frac{\beta I^*}{N} + \delta\right)\lambda + \frac{\beta K I^*}{N} = 0$, where $K = \gamma + aH + \delta$.

Here, we can apply Routh-Hurwitz Stability criteria, which states that for a quadratic, $\lambda^2 - a_1\lambda + a_2 = 0$, all roots have negative real parts if and only all the coefficients are positive, i.e. $a_1 > 0\ and\ a_2 > 0$.

In our case, $a_1 = \frac{\beta I^*}{N} + \delta$ and $a_2 = \frac{\beta K I^*}{N}$.

Since all the parameters $(N,\ \beta, \delta, K)$ are positive and at the endemic equilibrium $I^* > 0$, the coefficients a_1, a_2 are always positive.

Furthermore, if we write equation (19) as, $$A = \begin{pmatrix} -\left(\frac{\beta I^*}{N} + \delta\right) & -K \\ \frac{\beta I^*}{N} & 0 \end{pmatrix} = \begin{pmatrix} A_{11} & A_{12} \\ A_{21} & A_{22} \end{pmatrix}$$

Then its characteristic equation is, $\lambda^2 - (A_{11} + A_{22})\lambda + A_{11}A_{22} - A_{12}A_{21} = 0$

Therefore,

$$\lambda_1 = \frac{(A_{11} + A_{22}) + \sqrt{(A_{11} + A_{22})^2 - 4(A_{11}.A_{22} - A_{12}.A_{21})}}{2}$$

$$\lambda_2 = \frac{(A_{11} + A_{22}) - \sqrt{(A_{11} + A_{22})^2 - 4(A_{11}.A_{22} - A_{12}.A_{21})}}{2}$$

Where $(A_{11} + A_{22}) = -\left(\frac{\beta I^*}{N} + \delta\right)$ and $A_{11}.A_{22} - A_{12}.A_{21} = \frac{\beta K I^*}{N}$

Then, $\boldsymbol{E_2(S^*, I^*, R^*)}$ will be stable if $\lambda_1 < 0\ \ and\ \lambda_2 < 0$, i.e. if $(A_{11} + A_{22}) < 0\ \ and\ A_{11}.A_{22} - A_{12}.A_{21} > 0$.

since the $Trace(A) = -\left(\frac{\beta I^*}{N} + \delta\right)$, is always negative and $Det(A) = \frac{\beta K I^*}{N}$, is always positive, the two eigen values are both negative, i.e. $\lambda_1, \lambda_2 < 0$.

Therefore, the endemic equilibrium is locally asymptomatically stable whenever it exists, i.e. whenever $R_0 > 1$, where $R_0 = \frac{\beta}{\gamma + aH + \delta}$.

5. Numerical Analysis

For more practical approach of the model and to see the effects of healthcare capacity in real life situation, numerical methods are used for simulating the equilibria and analyze the different conditions for the stability of the equilibrium point. The objective here is to specify the effect of healthcare capacity in case of COVID-19 situation. For more realistic view of the model, the data for infection (given in figure1(a)), cured and death cases has been retrieved from PRS Legislative Research India website [17], to get some idea of rate of infection and basic reproduction number R_0 (figure 1(b)). The time series plot from the data collected shows distinct peaks and troughs corresponding to the three major waves of the pandemic. During early 2020 there was initial cases of infection and the rate of new infection was gradually increasing. The initial estimates of R_0 were high around 1.8 to 2.5. From mid 2020 to late 2020, the first wave of infection was slowly decreasing, due to healthcare facility and nation-wide lockdown. Here the estimated R_0 pushed down to 1.04 to less than 1. Then there was again

the second wave in the early 2021 to mid 2021and the estimated value rose to above 1 again. The third wave in the late 2021 to early 2022 was more intense with high peak with estimated R_0 was near to 2.98 but decline very quickly. From mid 2022 onwards there is a subsequent activity of infection rates, hovering near of slightly above the critical line, indicating localized outbreaks rather than a major national surge.

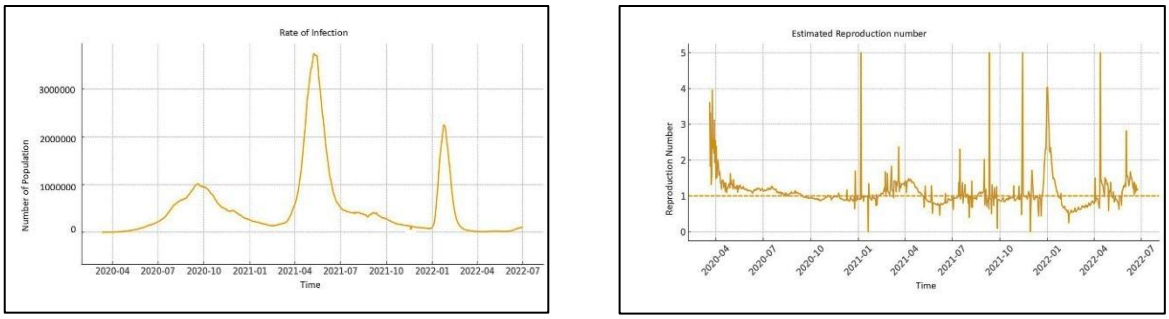

(a) (b)

Figure 1: (a) Infection rate of COVID-19 in India [17] (b) Estimated R_0 at different stages [17]

For mathematical simulation we use a hypothetical set of parameter values and see the changes in different condition.

Taking $N = 1000, \beta = 0.7, \gamma = 0.4, a = 0.001, H = 100, \delta = .1,\ \delta = \Lambda$ (for closed population) and solving the equations (5), (6) & (7), we get the feasible values of S, I & R as

$[S^* = 1000,\ I^* = 0.,\ R^* = 0.],\quad [S^* = 857.1428571,\ I^* = 23.80952381,\quad R^* = 119.0476190]$

Also, $R_0 = \frac{\beta}{\gamma + aH + \delta} = 1.167$, which means that the infection may increase depending upon the value of health care capacity and its effort.

5.1. For the point $E_1(S^*, 0, 0)$:

Case a: For, parameter values, $N = 1000, \beta = 0.7, \gamma = 0.4, a = 0.001, H = 100, \delta = .1,\ \delta = \Lambda,$

The corresponding Jacobian J_1 from equation (15), is $J_1 = \begin{pmatrix} -0.1 & -0.7 & 0 \\ 0 & 0.1 & 0 \\ 0 & 0.5 & -0.1 \end{pmatrix}$

Then the eigen values of J_1 is given by $det(J_1 - \lambda I) = 0$. Which gives $\lambda_1 = -0.1, \lambda_2 = 0.1, \lambda_3 = -0.1$.

Here not all eigen values are negative, i.e. $\lambda_1 < 0, \lambda_3 < 0, but\ \lambda_2 > 0$. which means that the disease-free equilibrium is not stable and if the disease is introduced into the population, the number of infected individuals will not converge back to zero.

Case b: Again, if we change the value of H by H=1100, and keep the other parameter values fixed and solve the equations (5), (6) and (7) we get the only feasible solution as, $[S^* = 1000,\ I^* = 0.,\ R^* = 0.]$.

And the Jacobian J_1 will change to $J_1 = \begin{pmatrix} -0.1 & -0.7 & 0 \\ 0 & -0.9 & 0 \\ 0 & 1.5 & -0.1 \end{pmatrix}$.

Therefore, the eigen-value of J_1, are $\lambda_1 = -0.1, \lambda_2 = -0.9, \lambda_3 = -0.1$.

Here, $\lambda_1, \lambda_2, \lambda_3 < 0$, it implies that the disease-free equilibrium is stable around $E_1(S^*, 0,0)$, and the number of infections eventually dies. The reproduction number at this stage is $R_0 = \frac{\beta}{\gamma + aH + \delta} = 0.43<1$.

Since $R_0 < 1$, the disease will eventually fade away after a number of days.

5.2. For the point $E_2(S^*, I^*, R^*)$:

Again, using the same parameter values, $N = 1000, \beta = 0.7, \gamma = 0.4, a = 0.001, H = 100, \delta = .1,$ $\delta = \Lambda$.

Here as $I^* \neq 0$, the feasible solution we get from equations (5), (6) & (7) is $[S^* = 857.1428571,\ I^* = 23.80952381,\ \ R^* = 119.0476190] \approx [S^* = 857,\ I^* = 24,\ \ R^* = 119]$

The corresponding Jacobian J_2 from equation (16), is

$$J_2 = \begin{pmatrix} -\left(\frac{\beta I^*}{N} + \delta\right) & -(\gamma + aH + \delta) & 0 \\ \frac{\beta I^*}{N} & 0 & 0 \\ 0 & \gamma + aH & -\delta \end{pmatrix} = \begin{pmatrix} -0.0168 & -0.6 & 0 \\ 0.0168 & 0 & 0 \\ 0 & 0.5 & -0.1 \end{pmatrix}$$

Then the eigen values of J_2 is given by $det(J_2 - \lambda I) = 0$ i.e. $\begin{vmatrix} -0.0168 - \lambda & -0.6 & 0 \\ 0.0168 & 0 - \lambda & 0 \\ 0 & 0.5 & -0.1 - \lambda \end{vmatrix} = 0,$

i.e. $(-0.1 - \lambda)(\lambda^2 + 0.0168\lambda + 0.01008) = 0$

i.e. $\lambda_1 = -0.1,\ \lambda_2 \approx -0.0084 + 0.10005i\ , \lambda_3 \approx -0.0084 - 0.10005i$

Here we can see that, $\lambda_1 < 0$ and λ_2, λ_3 have negative real part, which indicates that the disease persists around the equilibrium point. The non-zero imaginary part in the values of λ_2 and λ_3 indicates that the system's trajectory near the endemic equilibrium point will exhibit oscillatory behavior, i.e. the disease persists in natural cycle of outbreak. In the real world COVID-19 epidemic context, this suggests a cycle of outbreaks where the infected population might peak, then drop below the equilibrium, then rise again creating a sustained periodic pattern near the equilibrium point. Then there will be outbreak with waves of infection, but each wave will be smaller than the last until the disease eventually dies out depending upon the value of basic reproduction number at each stage of waves. At this point health care capacity play a crucial role for prevention of the outbreak.

To get the actual behavior of the pandemic, the actual data has been taken from PRS Legislative Research India website [17], (shown in figure 1 & figure 2) showing infection per day and the estimated reproduction number and fitted the data to check the effect on infection rates for different value of healthcare capacity (H) and healthcare efforts (a).

Now, for $N = 4000000, \beta = 0.3, \gamma = 0.2, \delta = .1,\ \delta = \Lambda$, the numerical simulation has been conducted for different values of a and H. Table below shows the extract of the numerical calculation for basic reproduction number for different healthcare values.

Table 1: *Table showing the change in the value of R_0 when we vary the value of healthcare capacity*

Parameter value	**Value range**	I^*	S^*	R_0	**Outbreak level**
$H = 0.1$	Low	177333	1716738	2.33	High endemic, there will be rapid accumulation with higher peak.
$H = 1000$	Medium	999999	2285714	1.75	Moderate endemic level and chances of accumulation over time.
$H = 5000$	High	0	4000000	0.875	Small outbreak and then stops.

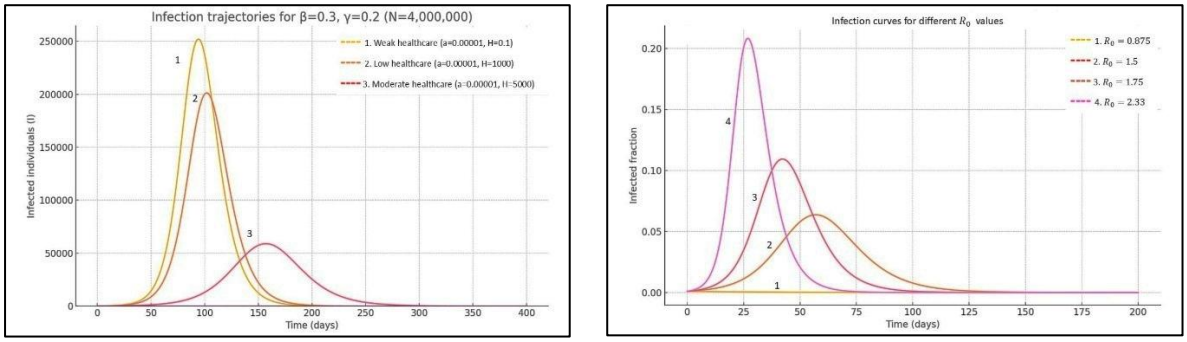

(a) (b)

Figure 2: (a) Infection trajectories for different H taking $\beta = 0.3$ & $\gamma = 0.2$. (b) infection trajectories for different R_0.

Which confirms the inherent dynamics of the system and when we include the healthcare capacity at the increasing rate of infection and its efforts can eventually lead to damped epidemic cycle near the equilibrium.

With mathematical simulation, the actual data of COVID-19 was fitted with the model, taking infection rate, $\beta = 1.3875$ per day and recovery rate, $\gamma = 1.3313$, shown in **figure 3(a)**.

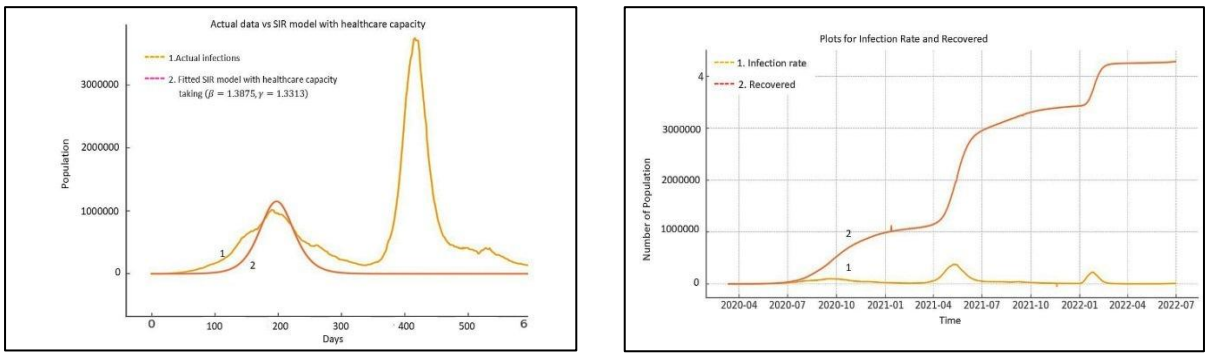

(a) (b)

Figure 3: (a) Actual infection with fitted SIR model (b) infection and recovered cases of COVID-19 pandemic in India [17].

From figure 3(a) we can see that the COVID-19 pandemic in India has several waves and three distinct peaks, but the infection curve from the model has only one. This is because we kept the rate of transmission rate, $\beta = 1.3875$ per day and recovery rate, $\gamma = 1.3313$ fixed. And due to the presence of healthcare capacity the infection rate gone down to zero. But in reality, the value of β and γ changes overtime which results in the fluctuation in the infection rates.

6. Conclusion

The COVID-19 pandemic presented unprecedented challenges, and the development of advanced epidemiological models is crucial for effective disease management. By integrating the prey-predator framework into the SIR model taking healthcare capacity as predator and infections as prey offers a promising avenue for a more comprehensive and realistic understanding of COVID-19 transmission, empowering public health officials and policymakers with valuable insights to navigate future pandemics.

The numerical simulation taking the different values of the parameter has been evaluated which generated different plots showing the time evolution of the susceptible, infected, recovered, and

deceased populations based on the specified parameters and initial conditions. At the equilibrium point of the healthcare capacity and infection model, the long-term behaviours of both infection levels and healthcare resources become stabilized, provided the system parameter meet the required conditions for coexistence and stability. Specifically, if healthcare capacity is sufficient relative to infection growth, the infection is controlled without overwhelming the system and both the healthcare resources and infection levels reach positive, steady values.

This outcome demonstrates that with a properly balanced system, where healthcare interventions can consistently match or exceed the infection rate, the disease persist at manageable levels and healthcare resources maintain their effectiveness over time. However, if the basic reproduction number exceeds the critical threshold, the infection can become endemic and persist within the population. Conversely if the interventions are highly effective and the basic reproduction number falls below unity, the infection will eventually die out and the system moves towards disease free equilibrium. However, we have demonstrated the model for healthcare capacity as predator and infection as prey taking healthcare capacity as constant parameter and taking total number of population constant, so, our future project will be to study the above system taking dynamic population and healthcare capacity.

End Notes

1. Cooper, I., Mondal A. & Antonopoulos C. G., (2020), "A SIR model assumption for the spread of COVID-19 in different communities", *Chaos, Solitons and Fractals*, Vol. 139, pp. 1-14.

2. Chen, Y.C., Lu, P.E. & Chang C. S., (2020), "A Time-Dependent SIR Model for COVID-19 with Undetectable Infected Persons", *IEEE transaction on network science and engineering.* vol. 7, No. 4, pp.3279-3294.

3. Mohajan, H. K., (2022), "Mathematical Analysis of SIR Model for COVID-19 Transmission*".* *Journal of Innovations in Medical Research*, Vol. 1, No. 2. pp. 1-18.

4. Rakshit, P., Kumar, S., Noeiaghdam S., Fernandez-Gamiz, U., Altanji, M.& Santra, S. S., (2022), "Modified SIR model for COVID-19 transmission dynamics: Simulation with case study of UK, US and India". Results in Physics. vol. 40. pp. 2211-3797.

5. Kangalgil, F., Topsakal, N. & Kuzucu, O., (2025), "Local dynamic analysis of the COVID-19 mathematical model based on discrete-time predator-prey population model". Turkish Journal of Mathematics. Vol. 49, pp. 139-156.

6. Kartal, N. & Kartal, S. (2023), "Complex dynamics of COVID-19 mathematical model on Erdős–Rényi network", *International Journal of Biomathematics*. Vol. 16(5). pp. 1-19.

7. Matouk, A.E., (2020), "Complex dynamics in susceptible-infected models for COVID-19 with multi- drug resistance". *Chaos, Solitons Fractals.* Vol. 140. pp. 1-13.

8. Vinitskya, S. I., Guseva, A. A., Derbovc, V. L., Krassovitskiyd, P. M., Pen'kove, F. M., & Chuluunbaatara, G., (2021), "Reduced SIR Model of COVID-19 Pandemic (2020)". *Computational Mathematics and Mathematical Physics*, Vol. 61, No. 3, pp. 376–387.

9. Dunn, P. R. & Hovel, K.A., (2019), "Predator type influences the frequency of functional responses to prey in marine habitats". *Biology letters – the royal society of publishing*. Vol. 16, pp. 1-18.

10. Sahoo, B. & Poria, S., (2014), "Diseased prey predator model with general Holling type interactions". *Applied mathematics and computation*, Vol. 226, pp. 83-100.

11. Konpola, A. A., (2021), "Evolution of COVID-19 disease using a one prey two predator model". *Advances in technology. Vol.1(1),* pp. 25-40.

12. Bozkurt, F., Yousef, A. & Abdeljawad T., (2020), "Analysis of the outbreak of the novel coronavirus COVID-19 dynamic model with control mechanisms", *Results Physics.* Vol. 2(19) . pp. 1-29.

13. Ali, A. (2017), "Bifurcation and chaos in a discrete time predator-prey system of Lessie type with generalized Holling type III functional response". *Journal of Applied Analysis and Computation*. Vol. **7**(2), pp. 411–426

14. Liu, B., Teng, Z. & Chen, L., (2005) "Analysis of a predator–prey model with Holling II functional response concerning impulsive control strategy". *Journal of Computational and Applied Mathematics.* Vol. 193. pp. 347–362.

15. Ali, N., Haque, M., Venturino, E. & Chakravarty, S., (2017), "Dynamics of a three species ratio-dependent food chain model with intra-specific competition within the top predator". *Computational Biology & Medicine,* Vol. 85. pp. 63–74.

16. Basu, S. & Campbell, R.H., (2020) "Going by the numbers: learning and modelling COVID- 19 disease dynamics". *Chaos Solitons Fractals*. Vol. 138. pp. 1-16.

17. The data of COVID-19 pandemic retrieved from PRS Legislative Research India website, https://prsindia.org/covid-19/overview .

18. Khan, M. H., Ahmed, M. & Alam, S.M.M., (2023), "Optimal control of an SIRD model with data-driven parameter estimation". *Results in Control and Optimization*. Vol. 14. pp. 2666-7207.